MODAL ANALYSIS OF SOME STRUCTURES USING CIRCLE - FIT METHOD

by

H. R. NIRANJANA MURTHY

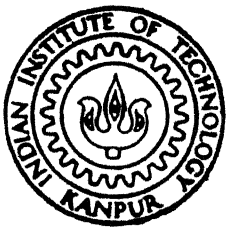

DEPARTMENT OF MECHANICAL ENGINEERING

INDIAN INSTITUTE OF TECHNOLOGY, KANPUR

FEBRUARY, 1988

MODAL ANALYSIS OF SOME STRUCTURES USING CIRCLE - FIT METHOD

A Thesis Submitted
In Partial Fulfilment of the Requirements
for the Degree of

MASTER OF TECHNOLOGY

by

H. R. NIRANJANA MURTHY

to the

DEPARTMENT OF MECHANICAL ENGINEERING
INDIAN INSTITUTE OF TECHNOLOGY, KANPUR

FEBRUARY, 1988

ME-1988-M-MUR-MOD

26/2/88

CERTIFICATE

This is to certify that the thesis entitled 'MODAL ANALYSIS OF SOME STRUCTURES USING CIRCLE-FIT METHOD' by H.R. Niranjana Murthy is a bonafide record of work done by him under my guidance and supervision for the award of the degree of Master of Technology at the Indian Institute of Technology, Kanpur. The work carried out in this thesis has not been submitted elsewhere for the award of a degree.

Bhupinder Pal Singh. Feb 26 88

(Dr. BHUPINDER PAL SINGH)
Assistant Professor
Department of Mechanical Engineering
I.I.T. Kanpur-208016

ACKNOWLEDGEMENT

I acknowledge with sincerity and gratitude, the guidance provided by Dr. Bhupinder Pal Singh in sorting out various problems through out the course of this thesis. I thank him for his contributions made by way of timely advices and criticisms.

I would like to express my sincere gratitude and thanks to Dr. V. Sundararajan for suggesting the topic of the thesis.

I thank Mr. H.V.C. Srivastava for his careful and neat typing of this thesis.

H.R. Niranjana Murthy

Feb. 25, 1988
I.I.T. Kanpur

CONTENTS

LIST OF TABLES

LIST OF FIGURES

NOMENCLATURE

c	Viscous damping coefficient
$[C]$	Viscous damping matrix
r^{D}_{jk}	Diameter of modal circle
$f(t)$	Excitation force
h	Hysteretic damping coefficient
$[H]$	Hysteretic damping matrix
Im	Imaginary part
j,k	Coordinates
k	Stiffness
k_r	Modal or generalized stiffness
$[K]$	Stiffness matrix
m	Mass
m_r	Modal or generalized mass
$[M]$	Mass matrix
N	Number of DOF in MDOF system
r	Mode number
Re	Real part
$\bar{\omega}$	Undamped system natural frequency of SDOF
$\bar{\omega}_r$	Undamped system natural frequency

ω	Excitation frequency
x	Displacement
$[Y(\omega)], y_{jk}$	Mobility matrix, function
$\dot{}$	Velocity (first time derivative)
$\ddot{}$	Acceleration (second time derivative)
$[\alpha(\omega)], \alpha_{jk}$	Receptance matrix, function
β , β'	Constants
γ , γ'	Constants
η_r	Hysteretic damping loss factor
ζ_r	Viscous damping ratio
$\{\Psi\}_r$	Eigen vector/mode shape
$[\Psi]$	Modal matrix
$\{\phi\}_r$	Mass-normalized eigen vector/mode shape
$[\phi]$	Mass-normalized modal matrix
$[\ ]$	Square matrix
$\{\ \}$	Column matrix
$\lfloor\ \rfloor$	Row matrix
ρ	Principal coordinates
τ, θ	Angles

ABSTRACT

Modal analysis of some discrete and continuous structures has been performed in the present work.Circle fit method is adopted for the analysis. Analysis has been done for structures with viscous/structural proportional damping. The results of the identified system parameters (mass and stiffness distributions) have been compared with the actual values. The close agreement between identified and actual values is shown.

CHAPTER -I

INTRODUCTION

The dynamic behaviour of real life structures are difficult to be analysed theoretically because of their complex geometry and uneven distribution of spatial parameters (mass, damping, stiffness). Even for the cases for which analytical and numerical solutions are possible, the nature of simplifications made necessitates an experimental verification. Modal analysis is one such method which is increasingly being employed for identification and validation of dynamic properties of physical systems.

Modal analysis involves the testing of structures with the aim of obtaining a mathematical description of their dynamic and vibration behaviour. The mathematical description could be an estimation of natural frequency and damping factor in some cases and the full evaluation of mass, stiffness and damping distribution in other cases. The method involves test-structure excitation to obtain the modal responses like receptance, mobility, etc., and the extraction of system model from the test data. The entire procedure is sometimes also referred to as modal testing.

1.1 REVIEW OF PREVIOUS WORK

A good review of the literature on modal analysis is given by Kundra [1]. Vepa [2] has recently reviewed modal identification methods and presented some of the inadequacies of the method. The topic of modal testing is neatly dealt with in a text by Ewins [3].

One of the earliest and pioneer paper in the development of the subject is of Kennedy and Pancu [4]. They presented a circle fit method for the system identification. Bishop and Gladwell [5] presented a state of the art theory of resonance testing which at that time was considerably in advance of its practical implementation. Salter [6] presented a relatively non-analytical approach to the interpretation of the measured data. Salter's approach, even though involving a good skill on the part of experimenter,gave a considerable insight into the vibration of structures.

After 1970, owing to the great advancement in instrumentation, considerable progress has been achieved. A bibliography of several such works is given in [7,8]. A few of the important works are mentioned here. Flannelly et al [9] presented a theory to extract a complete physical model from multipoint sinusoidal excitation data. They assume that the structure has as many degree-of-freedom as the number of excitation points. Kundra [1]

has employed this method in his work. He presented the theory for the lumped mass matrices. Berman [10] , in his paper, proposed a procedure which made use of the data obtained by the single point excitation. This approach makes the use of one column of mobility matrices at different frequencies.

1.2 OBJECTIVE AND SCOPE OF PRESENT WORK

The aim of the present work is to identify the modal parameters for discrete as well as continuous structures with viscous/structural proportional damping by modal analysis. Mass matrices for continuous structures are identified as consistent mass matrices.

In the second chapter the theoretical aspects of the present method are discussed. The circle fit method, which is employed in the present work, is explained in detail.

In the third chapter, the identified system parameters like mass and stiffness distributions are compared with the actual values both for discrete and continuous structures with different dampings mentioned earlier. Conclusions are presented at the end.

CHAPTER- II

CIRCLE-FIT METHOD

This chapter describes the circle fit method of modal analysis for multidegree of freedom (MDOF) structures. To understand the theory of this method for MDOF structures, it is worth to review the basics of vibration of single degree of freedom (SDOF) structure and MDOF structures.

2.1 SDOF STRUCTURE

The SDOF structure is shown in Fig. 2.1. It consists of mass m, spring of stiffness k and massless damper with coefficient of viscous damping c or coefficient of hysteretic damping h, f(t) is the excitation force applied to the mass and x is the response of this mass.

Its equation of motion with viscous damping is

$$m\ddot{x} + c\dot{x} + kx = f(t) = Fe^{j\omega t} \qquad \ldots. (2.1)$$

Assuming its solution as $x=Xe^{j\omega t}$, one gets the response as

$$X = \frac{F}{(k-\omega^2 m)+j\omega c} \qquad \ldots. (2.2)$$

Thus receptance for SDOF structure is

$$\alpha(\omega) = \frac{x}{f} = \frac{1}{(k-\omega^2 m)+j\omega c} \qquad \ldots. (2.3)$$

and its phase is

$$\underline{/\alpha(\omega)} = \tan^{-1}\left(-\omega c/k-\omega^2 m\right) \qquad \ldots. (2.4)$$

And its mobility is

$$Y(\omega) = \frac{\dot{x}}{f} = j\omega\, \alpha(\omega) \qquad \ldots. (2.5)$$

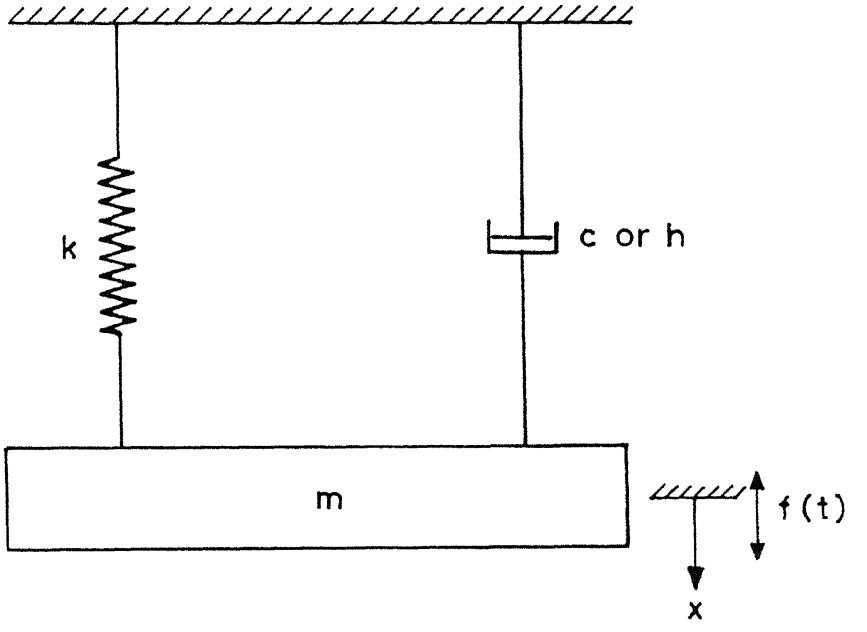

Fig. 2.1 SDOF structure.

It may be noted that receptance and mobility are complex quantities. Viscous damping model does not closely represent the real structures. Most of these structures when subjected to cyclic loading exhibit a stress-strain relationship which is a closed loop known as hysteresis loop. The energy dissipated per cycle due to this internal friction is proportional to the area of the hysteresis loop. Thus this damping is known as hysteretic or structural damping. This internal friction (structural damping) is found to be independent of frequency and is proportional to the displacement over a significant frequency range [11]. Since energy is dissipated, this damping force must be in phase with the velocity. Thus for simple harmonic motion, the damping force is given by jhx, where h is hysteretic damping coefficient. Equation of motion (2.1) for this hysteretic damping becomes

$$m\ddot{x} + jhx + kx = Fe^{j\omega t} \qquad \ldots\ (2.6)$$

Receptance for this case is

$$\alpha(\omega) = \frac{X}{F} = \frac{1}{(k-\omega^2 m+jh)} \qquad \ldots\ (2.7)$$

For modal analysis purposes the receptances and mobilities, which are complex quantities arepreferably given in the Nyquist or Argand plots. Mobility response for viscously damped case and receptance response for hysterically damped case are given in Fig. 2.2 and are exact circles, proved as follows:

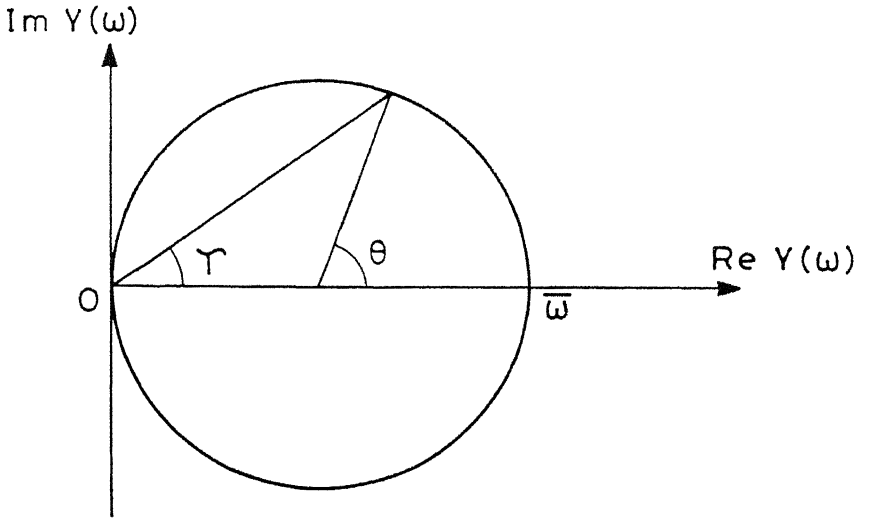

(a) Mobility response with viscous damping

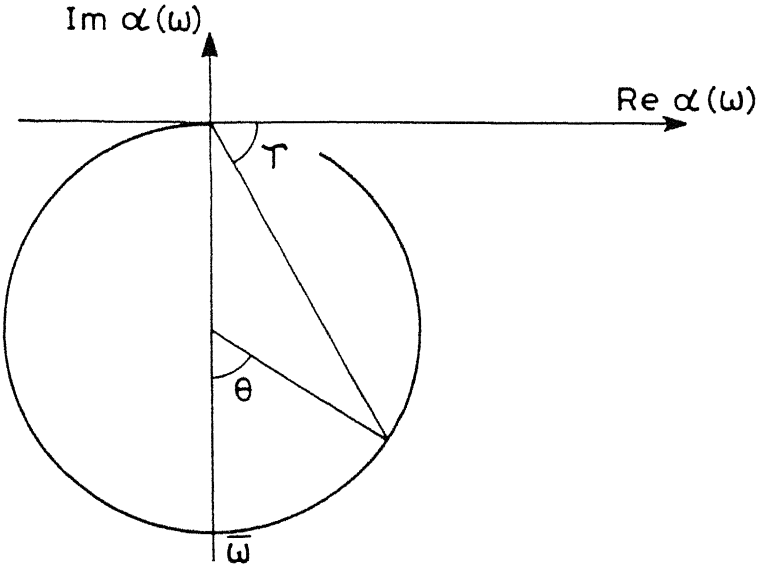

(b) Receptance response with structural damping

Fig. 2.2 Nyquist plot for SDOF system.

Equation (2.5) gives the mobility response as

$$Y(\omega) = \frac{j\omega}{(k-\omega^2 m)+ j\omega c} \qquad \ldots\ (2.8)$$

This can be rearranged as

$$Y(\omega)= \frac{\omega^2 c}{(k-\omega^2 m)^2+(\omega c)^2} + j \frac{\omega(k-\omega^2 m)}{(k-\omega^2 m)^2+(\omega c)^2}$$

or $$Y(\omega) = Re + j\ Im \qquad \ldots\ (2.9)$$

It can be seen that

$$(Re - \frac{1}{2c})^2 + Im^2 = (\frac{1}{2c})^2 \qquad \ldots\ (2.10)$$

Thus the mobility response plot for viscously damped SDOF structure is an exact circle with radius (1/2c) and centre as (Re= $\frac{1}{2c}$, Im= 0), Fig. 2.2(a).

Equation (2.7) gives the receptance response as

$$\alpha(\omega) = \frac{1}{k-\omega^2 m + jh}$$

This is rearranged as

$$\alpha(\omega) = \frac{(k-\omega^2 m)}{(k-\omega^2 m)^2+ h^2} + j \frac{(-h)}{(k-\omega^2 m)^2 + h^2}$$

or $$\alpha(\omega)= Re + j\ Im \qquad \ldots\ (2.11)$$

Real and imaginary parts are related as

$$Re^2 + (Im + \frac{1}{2h})^2 = (\frac{1}{2h})^2 \qquad \ldots\ (2.12)$$

Thus the receptance response plot for structurally damped SDOF structure is also an exact circle with radius as (1/2h) and centre as(Re=0,Im= $-\frac{1}{2h}$), Fig. 2.2(b). It may be noted that receptance and accelerance Argand plots for viscously damped case, and mobility and accelerance Argand plots for hysteretically damped case, are not exact circles but are circleslike.

The next step is to find the expression for damping by analysizing the modal circles. Considering the viscously damped case, it is observed from the Fig. 2.2(a) and the Eqn. (2.9) that,

$$\tan\tau = \tan\left(\frac{\theta}{2}\right) = \frac{k-\omega^2 m}{\omega c} = \frac{\bar{\omega}^2-\omega^2}{(\omega c/m)} \qquad \ldots\ (2.13)$$

If one takes two points $\theta_b = 90^\circ$, below natural frequency and $\theta_a = 90^\circ$ above natural frequency as in Fig. 2.4(a), one can write the following using Eqn. (2.13)

$$1 = \frac{\bar{\omega}^2-\omega_b^2}{c\omega_b/m}$$

$$1 = \frac{\omega_a^2-\bar{\omega}^2}{c\omega_a/m}$$

Adding above equations one gets

$$c = \frac{\omega_a - \omega_b}{m} \qquad \ldots\ (2.14)$$

Extending the same procedure to structurally damped system, one can write the following, by considering Eqn. (2.11) and Fig. 2.2(b)

$$\tan\tau = \frac{h/m}{(\bar{\omega}^2-\omega^2)}$$

and $\tan \theta/2 = \tan(90-\tau) = \dfrac{(\bar{\omega}^2-\omega^2)}{h/m}$ .... (2.15)

If one takes two points, one $\theta_b = 90^o$ below natural frequency $\bar{\omega}$ and other $\theta_a=90^o$ as shown in Fig. 2.4(b) above natural frequency, then using Eqn. (2.15), one obtains

$$\frac{\bar{\omega}^2 - \omega_b^2}{h/m} = 1$$

$$\frac{\omega_a^2 - \bar{\omega}^2}{h/m} = 1$$

Adding above equations, one gets

$$\omega_a^2 - \omega_b^2 = 2\frac{h}{m} = 2\frac{h\bar{\omega}^2}{k}$$

or $$\frac{h}{k} = \frac{\omega_a^2-\omega_b^2}{2\bar{\omega}^2}$$ .... (2.16)

2.2 MDOF STRUCTURES

In this section basics of vibration of MDOF are reviewed.

2.2.1 FREE UNDAMPED VIBRATIONS

The equations of motion for an undamped case, expressed in matrix form are

$$[M] \{\ddot{x}\} + [K] \{x\} = \{0\}$$ .... (2.17)

Here brackets [ ] stand for square matrices and braces { } stand for column matrices. Assuming $\{x\} = \{X\} e^{j\omega t}$, the above equation reduces to

$$[K] \{X\} = \omega^2 [M] \{X\}$$ .... (2.18)

which is an eigen equation.

Solving above equation, one gets eigen values ($\bar{\omega}_r^2$) and eigen vector matrix $[\Psi]$.

The eigen vectors possess a very important and useful property known as Orthogonality property [12]. This is not an ordinary orthogonality, but an orthogonality with respect to mass matrix $[M]$ as well as to stiffness matrix $[K]$, and is

$$\lfloor \Psi \rfloor_s [M] \{\Psi\}_r = 0 \qquad r \neq s \qquad \ldots\ (2.19)$$

$$\lfloor \Psi \rfloor_s [K] \{\Psi\}_r = 0 \qquad r \neq s$$

Here brackets $\lfloor\ \rfloor$ stand for row matrix.

The above equations show

$$[\Psi]^T [M] [\Psi] = [\bar{m}_r]$$
$$[\Psi]^T [K] [\Psi] = [\bar{k}_r] \qquad \ldots\ (2.20)$$

where $[\bar{m}_r]$ and $[\bar{k}_r]$ are diagonal matrices.

Eigenvectors $[\Psi]$ can be normalized as $[\phi]$,

$$[\phi] = [\Psi] [\bar{m}_r]^{-\frac{1}{2}} \qquad \ldots\ (2.21)$$

Then

$$[\phi]^T [M] [\phi] = [\bar{I}]$$
$$[\phi]^T [K] [\phi] = [\bar{\omega}_r^2] \qquad \ldots\ (2.22)$$

2.2.2 FREE DAMPED VIBRATIONS

All structures have some damping. For analysis purpose it is modelled as viscous, hysteretic, coulomb, aerodynamic etc. Generally it is difficult to determine which model is more appropriate for a given structure. Analysis becomes quite simple if viscous and hysteretic damping are proportional to stiffness and mass, i.e.

$$[C] = \beta'[K] + \gamma'[M]$$
$$[H] = \beta\,[K] + \gamma\,[M] \qquad \ldots\ (2.23)$$

This assumption has been used in this work.

Equation of motion for viscous damping becomes

$$[M]\{\ddot{x}\} + (\beta'[K] + \gamma'[M])\{\dot{x}\} + [K]\{x\} = \{0\} \qquad \ldots\ (2.24)$$

Using coordinate transformation $\{x\} = [\Psi]\{\rho\}$ .... (2.25)
and premultiplying by $[\Psi]^T$, the Eqn. (2.24) becomes

$$[\tilde{m}_r]\{\ddot{\rho}\} + (\beta'[\tilde{k}_r] + \gamma'[\tilde{m}_r])\{\dot{\rho}\} + [\tilde{k}_r]\{\rho\} = \{0\} \qquad \ldots\ (2.26)$$

The r-th equation is

$$m_r\,\ddot{\rho}_r + (\beta'\,k_r + \gamma' m_r)\,\dot{\rho}_r + k_r\,\rho_r = 0$$

or

$$\ddot{\rho}_r + 2\zeta_r\bar{\omega}_r\dot{\rho}_r + \bar{\omega}_r^2\rho_r = 0 \qquad \ldots\ (2.27)$$

where $\bar{\omega}_r^2 = \frac{k_r}{m_r}$, $\zeta_r = \frac{1}{2} \frac{(\beta' k_r + \gamma' m_r)}{\sqrt{k_r m_r}} = \frac{1}{2} \beta' \bar{\omega}_r + \gamma'/2\bar{\omega}_r$

.... (2.28)

Equation of motion for hysteretic damping is

$$[M]\{\ddot{x}\} + j(\beta [K] + \gamma [M])\{x\} + [K]\{x\} = \{0\}$$

.... (2.29)

Proceeding as above, this equation reduces to

$$\ddot{\rho}_r + \bar{\omega}_r^2 (1 + j\,\eta_r)\rho_r = 0 \qquad \text{.... (2.30)}$$

where $\bar{\omega}_r^2 = \frac{k_r}{m_r}$, $\eta_r = \beta + \gamma/\bar{\omega}_r^2$ .... (2.31)

2.2.3 FORCED DAMPED VIBRATIONS

Equation of motion, for viscously damped case becomes

$$[M]\{\ddot{x}\} + (\beta'[K] + \gamma'[M])\{\dot{x}\} + [K]\{x\} = \{F\}\, e^{j\omega t}$$

.... (2.32)

Assuming $\{x\} = \{X\}\, e^{j\omega t}$, one gets

$$([K] - \omega^2 [M] + j\,\omega(\beta'[K] + \gamma'[M]))\{X\} = \{F\} \quad \text{.... (2.33)}$$

or $\{X\} = [\alpha(\omega)]\{F\}$

where

$$[\alpha(\omega)]^{-1} = ([K] - \omega^2 [M] + j\omega(\beta'[K] + \gamma'[M]))$$

.... (2.34)

For modal analysis, it is better to change this $[\alpha(\omega)]$ matrix in terms of modal properties. Premultiplying $[\alpha(\omega)]^{-1}$ by $[\Psi]^T$ and post-multiplying by $[\Psi]$ to obtain

$$[\Psi]^T [\alpha(\omega)]^{-1} [\Psi] = ([k_r]-\omega^2[m_r]+j\omega(\beta'[k_r]+\gamma'[m_r]))$$

Taking inverse on both sides, one gets

$$[\Psi]^{-1} [\alpha(\omega)] [\Psi]^{T^{-1}} = ([k_r] -\omega^2 [m_r]+j\omega(\beta'[k_r]+\gamma'[m_r]))^{-1}$$

Again premultiplying by $[\Psi]$ and post-multiplying by $[\Psi]^T$ gives

$$[\alpha(\omega)] = [\Psi] ([k_r] -\omega^2 [m_r]+j\omega(\beta'[k_r] +\gamma'[m_r]))^{-1} [\Psi]^T \quad \ldots. (2.35)$$

Typical coefficient of this matrix is

$$\alpha_{jk}(\omega) = \sum_{r=1}^{N} \frac{{}_r\Psi_j \; {}_r\Psi_k}{(k_r-\omega^2 m_r)+j\omega(\beta' k_r+\gamma' m_r)}$$

or

$$\alpha_{jk}(\omega) = \sum_{r=1}^{N} \frac{{}_r\phi_j \; {}_r\phi_k}{(\bar{\omega}_r^2-\omega^2)+j\omega(\beta' \bar{\omega}_r^2+\gamma')} \quad \ldots. (2.36)$$

where ${}_r\phi_j$ is the j-th element of r-th mode .

Equation of motion for hysteretic damping is

$$[M]\{\ddot{x}\} +j(\beta [K] +\gamma [M]) \{x\} +[K]\{x\}= \{F\} e^{j\omega t} \quad \ldots. (2.37)$$

Proceeding as above $[\alpha(\omega)]^{-1}$ matrix in this case is

$$[\alpha(\omega)]^{-1}= ([K] -\omega^2 [M] +j(\beta [K] +\gamma [M])) \quad \ldots. (2.38a)$$

and its typical coefficient is

$$\alpha_{jk}(\omega) = \sum_{r=1}^{N} \frac{{}_r\Psi_j \; {}_r\Psi_k}{(k_r - \omega^2 m_r) + j(\beta k_r + \gamma m_r)}$$

or

$$\alpha_{jk}(\omega) = \sum_{r=1}^{N} \frac{{}_r\phi_j \; {}_r\phi_k}{(\bar{\omega}_r^2 - \omega^2) + j(\beta\bar{\omega}_r^2 + \gamma)} \qquad \ldots\ldots (2.38b)$$

2.3 CIRCLE-FIT METHOD

This section describes the circle fit method for extracting natural frequencies, damping coefficients, mass and stiffness coefficients both for viscously damped and structurally damped cases. Firstly the effect of off-resonant contribution is briefed for structural damping case (same is true for viscous damping). Secondaly the procedure for modal parameter extraction is discussed.

Response of MDOF structures is given by Eqn.(2.33)

$$\{X\} = [\alpha(\omega)]\{F\}$$

where

$$\alpha_{jk}(\omega) = \sum_{r=1}^{N} \frac{{}_r\phi_j \; {}_r\phi_k}{(\bar{\omega}_r^2 - \omega^2) + j(\beta\bar{\omega}_r^2 + \gamma)} \qquad \ldots\ldots (2.38)$$

Equation (2.38) can be expressed as

$$\alpha_{jk}(\omega) = \frac{{}_r\phi_j \; {}_r\phi_k}{(\bar{\omega}_r^2 - \omega^2) + j(\beta\bar{\omega}_r^2 + \gamma)} + \sum_{\substack{s=1 \\ s\neq r}}^{N} \frac{{}_s\phi_j \; {}_s\phi_k}{(\bar{\omega}_s^2 - \omega^2) + j(\beta\bar{\omega}_s^2 + \gamma)} \qquad \ldots\ldots (2.39)$$

It is seen from this equation that in the vicinity of resonance ($\omega = \bar{\omega}_r$), the receptance is controlled by the first term in Eqn. (2.39) relating to the r-th mode. This term when drawn

in vicinity of $\omega=\bar{\omega}_r$ in Nyquist plot will be a circle like, Fig. 2.3(a) and second term (of series) giving the combined effects of all other modes is essentially constant through the narrow range of frequencies, $\omega_a-\bar{\omega}_r-\omega_b$, Fig. 2.3(b). Combined effect of two terms of the above equation is shown in Fig. 2.3(c), which is circle like. The greater the range of frequency over which the combined effect (off-resonant contribution) is constant, the greater will be the part of the curve coinciding with the circle. The circle is displaced by an amount determined by the combined effect of all other modes.

When once the modal circle is fitted using mobilities in case of viscous damping and receptances in case of structural damping, the next step is to determine the natural frequency of that mode. The natural frequency, in case of viscously damped system, is located where the real component is maximum on the modal circle as shown in Fig. 2.4(a). Similarly the natural frequency, in case of structurally damped system,is located where the imaginary component on the modal circle is maximum.

After locating the natural frequency, the next step is to estimate the damping of the mode under consideration.

Consider viscously damped case. The mobility expression by considering Eqn. (2.36), can be written as follows.

$$y_{jk}(\omega)= \frac{\omega^2(\beta'\bar{\omega}_r^2+\gamma')({}_r\phi_j\ {}_r\phi_k)}{(\bar{\omega}_r^2-\omega^2)^2+\omega^2(\beta'\bar{\omega}_r^2+\gamma')^2} + j\ \frac{\omega(\bar{\omega}_r^2-\omega^2)({}_r\phi_j\ {}_r\phi_k)}{(\bar{\omega}_r^2-\omega^2)^2+\omega^2(\beta'\bar{\omega}_r^2+\gamma')^2} \quad \ldots\ (2.40)$$

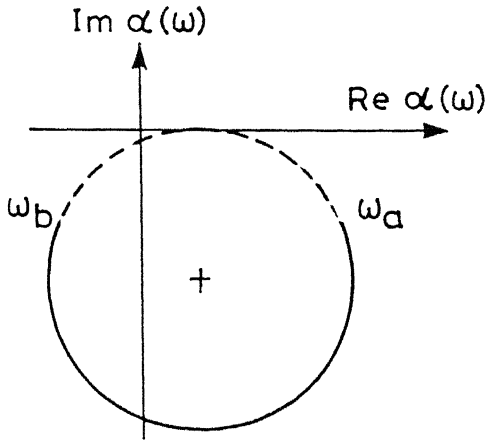

(a) First term of eqn. (2.35), near $\overline{\omega}_r$

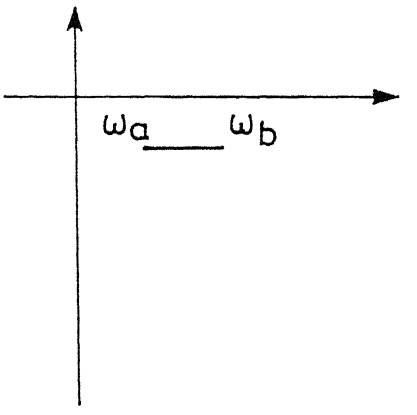

(b) Second term of eqn (2.35), near $\overline{\omega}_r$

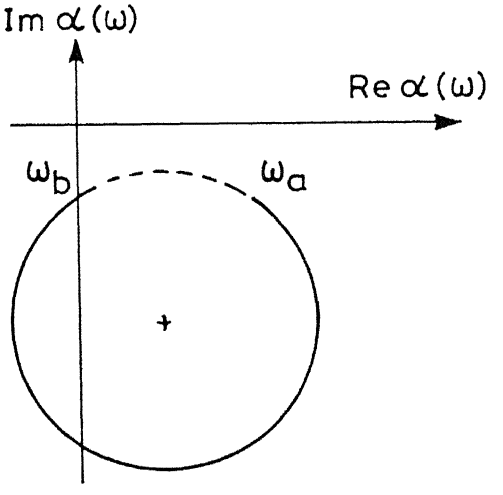

(c) Equation (2.35), near $\overline{\omega}_r$.

Fig. 2.3 Nyquist plot of MDOF structure.

Considering Fig. 2.2(a), one can express the angle τ as

$$\tan \tau = \tan(\theta/2) = \frac{(\bar{\omega}_r^2 - \omega^2)}{\omega(\beta' \bar{\omega}_r^2 + \gamma')} \quad \ldots\ (2.41)$$

Taking $\theta_b = 90^\circ$ (below natural frequency) and $\theta_a = 90^\circ$ (above natural frequency), Fig. 2.4(a)

$$1 = \frac{(\bar{\omega}_r^2 - \omega_b^2)}{\omega_b(\beta' \bar{\omega}_r^2 + \gamma')}$$

$$1 = \frac{\omega_a^2 - \bar{\omega}_r^2}{\omega_a(\beta' \bar{\omega}_r^2 + \gamma')}$$

Adding above equations, one gets

$$\beta' \bar{\omega}_r^2 + \gamma' = \omega_a - \omega_b$$

Using Eqn. (2.28), the above equation becomes

$$\zeta_r = \frac{\omega_a - \omega_b}{2\ \bar{\omega}_r} \quad \ldots\ (2.42)$$

Similarly considering structurally damped case, Eqn. (2.38) can be written as

$$\alpha_{jk}(\omega) = \frac{(\bar{\omega}_r^2 - \omega^2)({}_r\phi_j\ {}_r\phi_k)}{(\bar{\omega}_r^2 - \omega^2)^2 + (\beta \bar{\omega}_r^2 + \gamma)^2} - j\ \frac{(\beta \bar{\omega}_r^2 + \gamma)({}_r\phi_j\ {}_r\phi_k)}{(\bar{\omega}_r^2 - \omega^2)^2 + (\beta \bar{\omega}_r^2 + \gamma)^2}$$

$\ldots\ (2.43)$

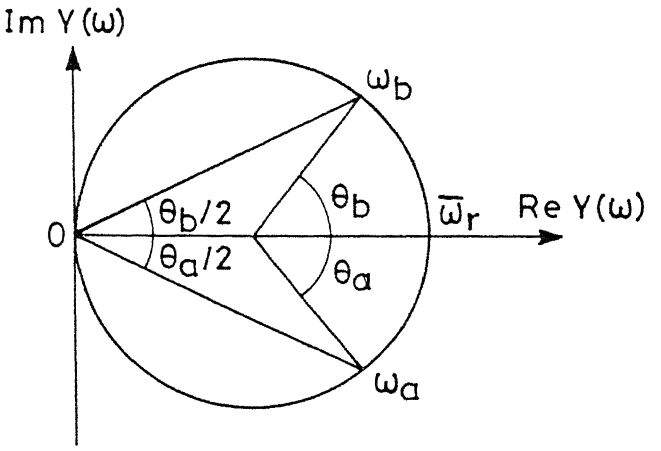

(a) Mobility plot

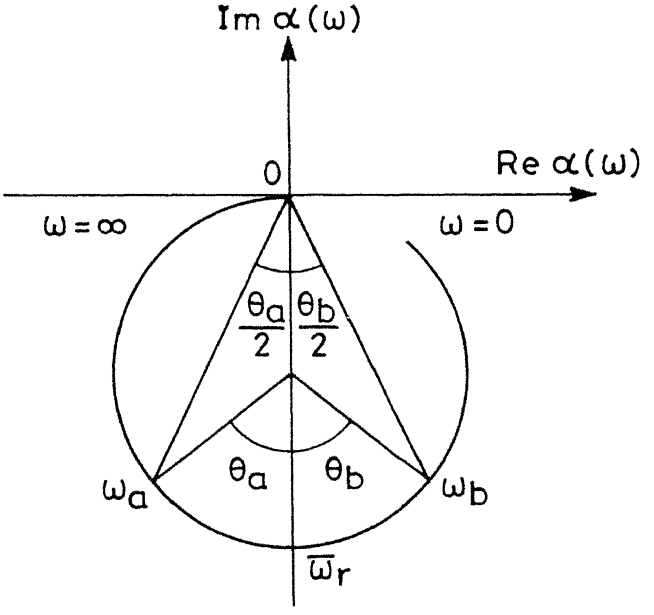

(b) Receptance plot

Fig. 2.4 Propeties of modal circle.

Considering Fig. 2.2(b), one gets the angle τ as

$$\tan \tau = \frac{\beta\bar{\omega}_r^2+\gamma}{\bar{\omega}_r^2-\omega^2}$$

or

$$\tan(\theta/2) = \tan(90-\tau) = \frac{\bar{\omega}_r^2-\omega^2}{\beta\bar{\omega}_r^2+\gamma} \quad \ldots\ (2.44)$$

Taking $\theta_b=90^o$ (below $\bar{\omega}_r$) and $\theta_a = 90^o$ (above $\bar{\omega}_r$) as shown in Fig. 2.4(b)

$$1 = \frac{(\bar{\omega}_r^2-\omega_b^2)}{(\beta\bar{\omega}_r^2+\gamma)}$$

$$1 = \frac{(\omega_a^2-\bar{\omega}_r^2)}{(\beta\bar{\omega}_r^2+\gamma)}$$

Adding above equations, one gets

$$2(\beta\bar{\omega}_r^2+\gamma) = \omega_a^2-\omega_b^2$$

Using Eqn. (2.31), the above equation becomes

$$\eta_r = \frac{(\omega_a^2-\omega_b^2)}{2\bar{\omega}_r^2} \quad \ldots\ (2.45)$$

After determining natural frequency ($\bar{\omega}_r$) and damping (ζ_r or η_r) at a given mode, the next step is to estimate the eigenvector $\{\bar{\phi}\}_r$ associated with that mode. This is done by linking the diameter of modal circle with other two quantities viz, natural frequency and damping.

Consider Eqn. (2.40) for viscously damped system substituting $\omega=\bar{\omega}_r$, one gets mobility as

$$y_{jk}(\omega)\Big|_{\omega=\bar{\omega}_r} = \frac{{}_r\phi_j\ {}_r\phi_k}{(\beta'\bar{\omega}_r^2+\gamma')} \qquad \ldots\ (2.46)$$

On observation, the above Eqn. contains only real part which is shown in Fig. 2.5(a). The magnitude of $y_{jk}(\omega)$ at $\omega=\bar{\omega}_r$ becomes the diameter $({}_rD_{jk})$ of the modal circle as the Eqn. (2.40) doesn't contain off-resonant terms. Rewriting above equation one gets

$${}_r\phi_j\ {}_r\phi_k = y_{jk}(\omega)\Big|_{\omega=\bar{\omega}_r}(\beta'\bar{\omega}_r^2+\gamma') = 2\ {}_rD_{jk}\ \bar{\omega}_r\ \zeta_r \qquad \ldots\ (2.47)$$

Considering the point response y_{11} at $\omega=\bar{\omega}_1$ one can compute ${}_1\phi_1$ (i.e. ϕ_{11}) and at $\omega=\bar{\omega}_2, \bar{\omega}_3, \ldots\ldots, \bar{\omega}_n$ one can compute ${}_2\phi_1, {}_3\phi_1, \ldots\ldots, {}_n\phi_1$ (i.e. $\phi_{12}, \phi_{13}, \ldots., \phi_{1n}$). Thus first row of the normalized eigenvector matrix $[\phi]$ is known. From transfer response y_{12} at $\omega=\bar{\omega}_1$ one can compute ${}_1\phi_1 \cdot {}_1\phi_2$ (i.e. $\phi_{11}\ \phi_{21}$), thus ϕ_{21} is known. Similarly coefficients $\phi_{22}, \phi_{23}, \ldots, \phi_{2n}$ are computed from transfer response y_{12} at $\omega=\bar{\omega}_2, \bar{\omega}_3, \ldots., \bar{\omega}_n$. Continuing this, the full normalized eigenvector matrix $[\phi]$ is determined.

Simiarly the modal quantities can be related with the diameter of modal circle in case of structurally damped systems as follows:

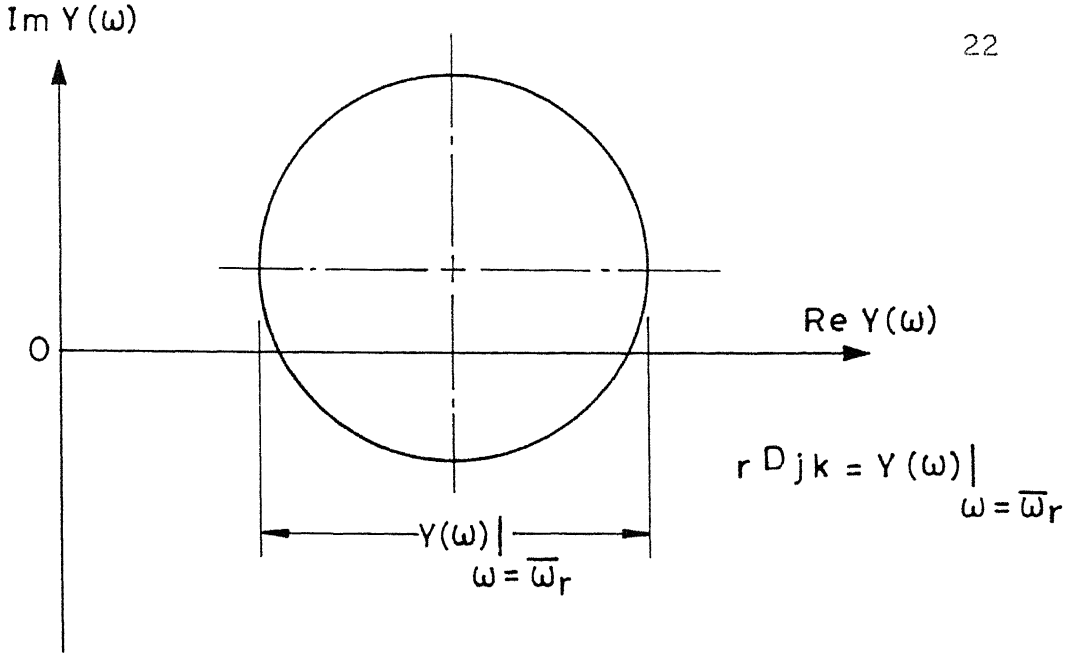

(a) Mobility plot

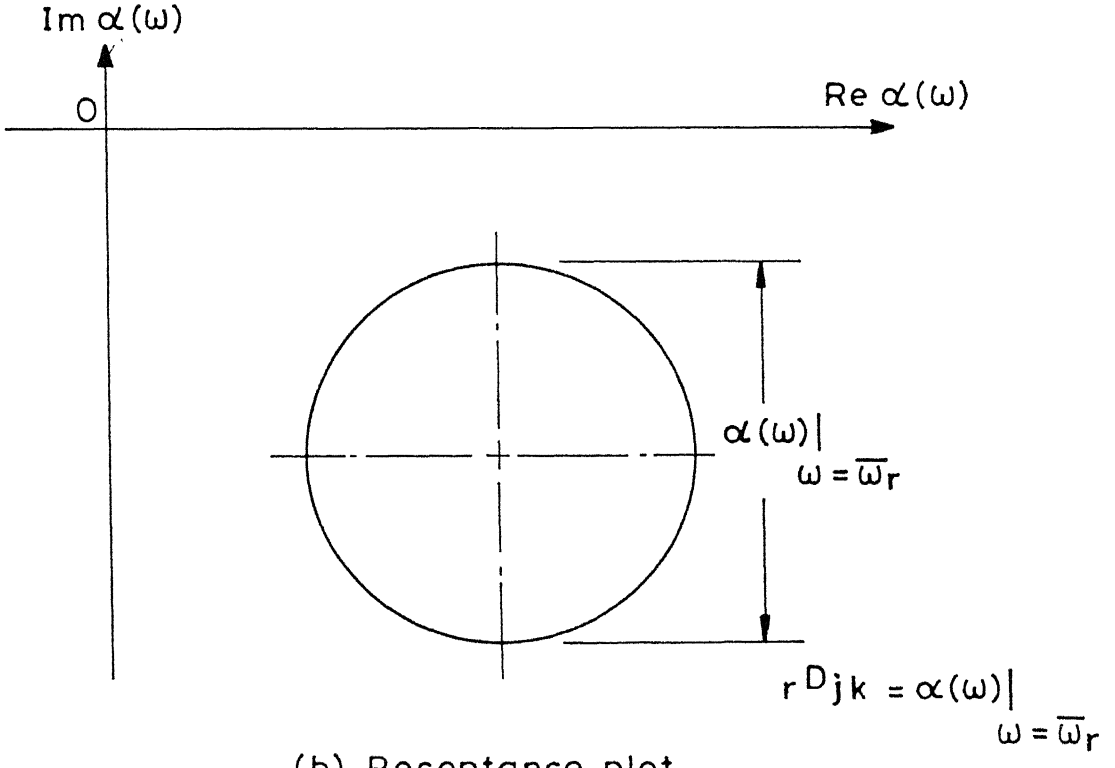

(b) Receptance plot .

Fig. 2.5 Plots at $\omega = \bar{\omega}_r$

Consider Eqn. (2.43) for structurally damped case. Substituting $\omega=\bar{\omega}_r$ one gets, receptance as

$$\alpha_{jk}(\omega)\Big|_{\omega=\bar{\omega}_r} = -j\,\frac{{}_r\phi_j\,{}_r\phi_k}{(\beta\bar{\omega}_r^2+\gamma)} \qquad \ldots\ (2.48)$$

On observation, one can know that the above equation contains only imaginary quantity, which is shown in Fig. 2.5(b). The magnitude of $\alpha_{jk}(\omega)$ at $\omega=\bar{\omega}_r$ is equal to the diameter $({}_rD_{jk})$ of the modal circle as the Eqn. (2.43) doesn't contain any terms pertaining to off-resonant contribution. Rewriting above equation, one gets

$${}_r\phi_j\,{}_r\phi_k = \alpha_{jk}(\omega)\Big|_{\omega=\bar{\omega}_r}(\beta\bar{\omega}_r^2+\gamma) = {}_rD_{jk}\,\eta_r\,\bar{\omega}_r^2 \qquad \ldots\ (2.49)$$

Normalized eigenvector matrix $[\phi]$ is determined as explained earlier for viscous damping case.

After knowing the modal matrix $[\phi]$, mass matrix $[M]$ and stiffness matrix $[K]$ are obtained from Eqn. (2.22) as

$$[M] = [\phi]^{-T}[\phi]^{-1}$$
$$[K] = [\phi]^{-T}[\bar{\omega}_r^2][\phi]^{-1} \qquad \ldots\ (2.50)$$

CHAPTER - III

RESULTS AND DISCUSSION

The first part of the present chapter discusses some of the assumptions made in the present analysis. In the latter part, the results obtained for the discrete and continuous systems with the structural/viscous damping are discussed.

3.1 MODELLING METHODOLOGY

In this section some of the simplifications made for the present analysis are explained below.

The Eqn. (2.19) gives the relationship of the damping matrices with the mass and stiffness matrices. For the present analysis, the damping matrices are considered to be proportional to the stiffness matrices only. Hence,

$$[C] = \beta'[K]$$
$$[H] = \beta[K] \qquad \ldots\ (3.1)$$

With this assumption, $\gamma=0$. The Eqns. (2.28) and (2.31) become

$$\zeta_\gamma = \frac{1}{2}\ \beta'\bar{\omega}_\gamma$$
$$\eta_\gamma = \beta \qquad \ldots\ (3.2)$$

As the experimental values of the modal response were not available, the receptance/mobility response information was generated from theoretical models (discrete and finite element models).

3.2 RESULTS AND DISCUSSIONS

Tables 3.1-3.14 document the actual and identified values of mass and stiffness matrices for the cases studied.

Figure 3.1 shows the two DOF system studied and Table 3.1 gives its actual mass and stiffness matrices. Theoretical receptance for structural damping ratio of 0.01 and 0.05 is calculated using Eqn. (2.38a). Mass and stiffness matrices are calculated from these using circle fit method. A comparision of results shows the close agreement between the actual and identified values. The identified mass is found to be almost diagonal, with the off-diagonal terms being small in comparision with the diagonal terms. The results for the case with a damping of 0.05 are closer than that of 0.01, as the response peaks are very well separated for the former case, thus making it easier to accurately select the range. This improves the quality of curve fit, thus making system identification more accurate.

Figure 3.2 shows an axial rod fixed at one end. First it was modelled as two finite elements and then as three finite elements. Consistent mass matrices were used. These matrices are given in Table 3.2-3.3. Structural damping factor taken were 0.01 and 0.05. Theoretical receptance was calculated using Eqn. (2.38a). Mass and stiffness coefficients were calculated from this using circle fit method. Identified values are given in Table 3.2-3.3.The identified values agree well with the actual values.

The beam with one end fixed is shown in Fig. 3.3. Here also it was modelled first as two finite elements and then as three finite elements with 2 DOF per node. Consistent mass matrices were used. Theoretical receptance was generated using Eqn.(2.38a). The mass and stiffness values were identified using circle fit method. Both assumed and identified values are given in Table 3.4-3.7 for structural damping factor 0.01 and 0.05. It is observed that the identified values agree closely with actual values.

Figure 3.4 shows L-Frame structure fixed at node 3. It was modelled as two elements with three DOF per node. Consistent mass matrices were used and theoretical receptance was generated using Eqn. (2.38a). Table 3.8-3.9 show the identified and actual values for structural damping factor 0.01 and 0.05. It is observed that the identified values are closer to actual values.

Figure 3.5 shows F-Frame structure fixed at node 5. It was modelled as 4 elements with three DOF per node. Consistent mass matrices were used. Theoretical receptance was generated using Eqn. (2.38a). The identified mass and stiffness values are shown in Table 3.10. The identified values are quite closer to actual values.

Some of the cases discussed earlier, were also analysed for proportional viscous damping. Consistent mass matrices were used. Theoretical receptance was generated using Eqn. (2.38a).

Later on, mobility was obtained from receptance for analysis. The modal parameters were extracted using circle fit method. The various cases analysed are discussed below.

Table 3.11 shows the actual and identified values for a two DOF discrete system, Fig. 3.1. The identified values agree well with actual values.

Table 3.12 shows the actual and identified values for an axial rod with two elements, Fig. 3.2(a). The identified values agree well with actual values.

Table 3.13 shows the identified and actual values for a beam with two elements, Fig. 3.3(a). The identified values agree well with actual values.

Table 3.14 shows the identified and actual values for L-Frame, Fig. 3.4. The identified value agree well with actual values.

3.3 CONCLUSION

From the present analysis it can be concluded that circle fit method gives fairly accurate identification of modal parameters for discrete as well as continuous structures with viscous/structural proportional damping.

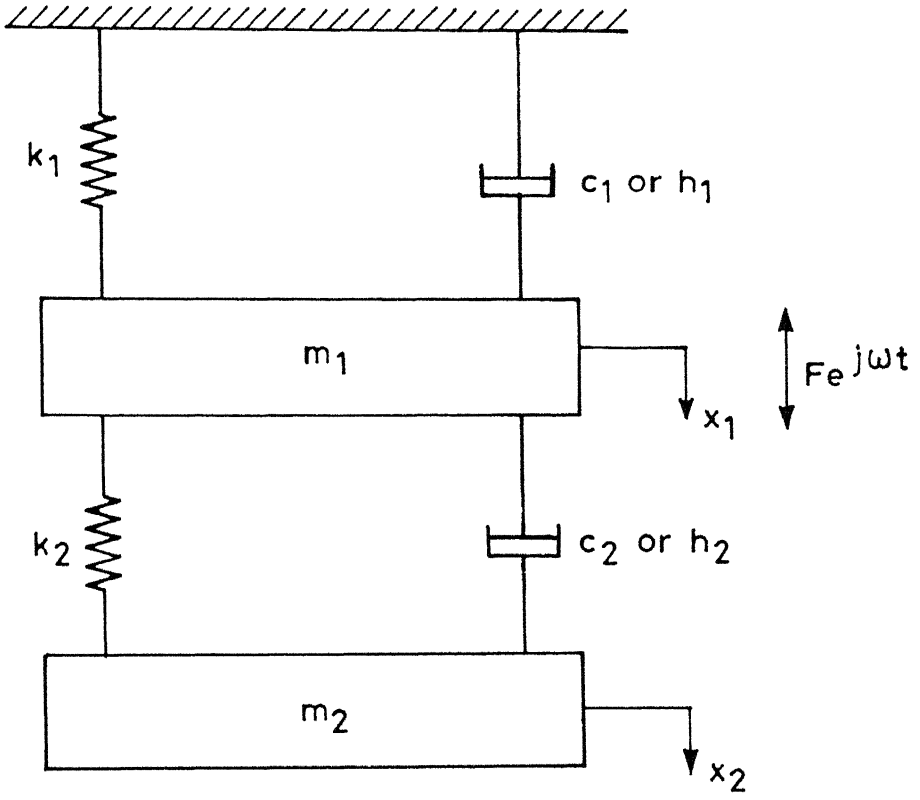

m_1 = 1.0 kg ; k_1 = 15.0 kN/m

m_2 = 2.0 kg ; k_2 = 20.0 kN/m

Fig. 3.1 Two DOF discrete system.

Table 3.1 Comparision for a discrete system (2x2) (structural damping)

	η=0.01			
	Actual values		Identified values	
Mass matrix	1.0000	0.0000	1.0148	-0.0009
	0.0000	2.0000	-0.0009	2.0496
Stiffness matrix x 10^{4}	3.5000	-2.0000	3.5464	-2.0496
	-2.0000	2.0000	-2.0496	2.0642

	η= 0.05			
	Actual values		Identified values	
Mass matrix	1.0000	0.0000	0.9992	-0.0039
	0.0000	2.0000	-0.0039	2.0132
Stiffness matrix x 10^{4}	3.5000	-2.0000	3.5079	-2.0061
	-2.0000	2.0000	-2.0061	2.0074

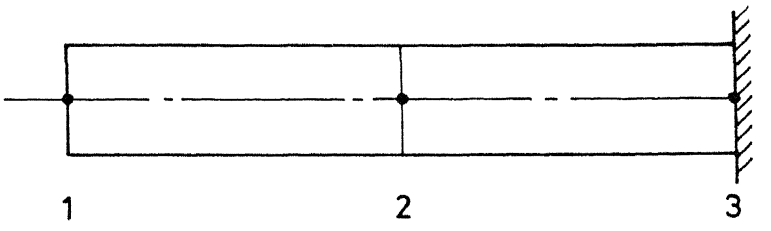

(a) Two elements

L	600 mm
A	625 mm^2
ρ	7800 kg/mm^3
E	207 GPa

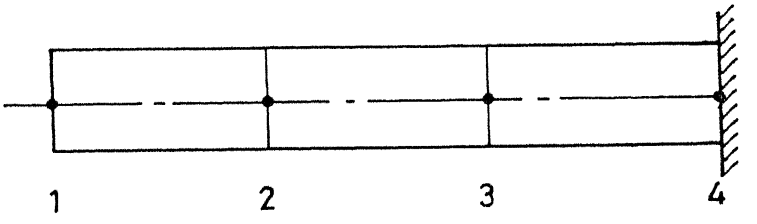

(b) Three elements

Fig. 3.2 Axial rod, finite elements.

Table 3.2 Comparision for an axial rod(2x2) (structural damping)

$\eta = 0.01$				
	Actual values		Identified values	
Mass matrix	5.1071	2.5535	5.0923	2.5305
	2.5535	1.0214	2.5305	1.0181
Stiffness matrix x 10^8	4.1250	-4.1250	4.1231	-4.1299
	-4.1250	8.2499	-4.1299	8.2455

$\eta = 0.05$				
	Actual values		Identified values	
Mass matrix	5.1071	2.5535	5.1066	2.5365
	2.5535	1.0214	2.5365	1.0133
Stiffness matrix x 10^8	4.1250	-4.1250	4.1172	-4.1164
	-4.1250	8.2499	-4.1164	8.2185

Table 3.3.Comparision for an axial rod (3x3) (structural damping)

	η= 0.01					
	Actual values			Identified values		
Mass matrix	3.4048	1.7024	0.0000	3.4156	1.7276	0.0088
	1.7024	6.8096	1.7024	1.7276	6.8307	1.7041
	0.0000	1.7024	6.8096	0.0088	1.7041	6.7993
Stiffness matrix x 10^8	6.1875	-6.1875	0.0000	6.1648	-6.1578	0.0066
	-6.1875	12.3749	-6.1875	-6.1578	12.3548	-6.1970
	0.0000	-6.1875	12.3749	0.0066	-6.1970	12.3799

	η= 0.05					
	Actual values			Identified values		
Mass matrix	3.4048	1.7024	0.0000	3.5106	1.8369	-0.0073
	1.7024	6.8096	1.7024	1.8369	6.7557	1.4670
	0.0000	1.7024	6.8096	-0.0073	1.4670	6.4820
Stiffness matrix x 10^8	6.1875	-6.1875	0.0000	6.0115	-6.0020	0.1061
	-6.1875	12.3749	-6.1875	-6.0020	12.2621	-6.3734
	0.0000	-6.1875	12.3749	0.1061	-6.3734	12.3558

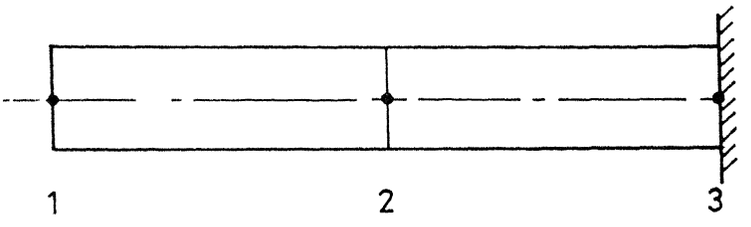

(a) Two elements

L	600 mm
A	625 mm^2
I	32552 mm^4
ρ	7800 kg/m^3
E	207 GPa

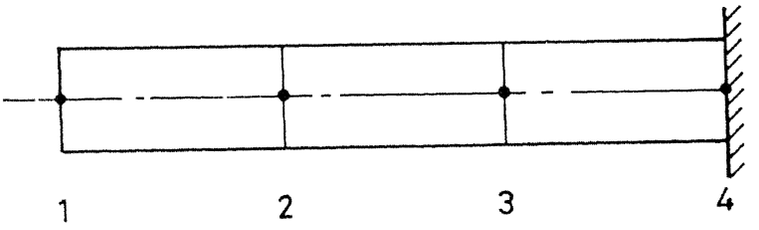

(b) Three elements

Fig. 3.3 Beam finite elements.

Table 3.4 Comparision for a beam (4x4) (structural damping)

	η= 0.01							
	Actual values				Identified values			
Mass matrix	0.5432	0.0230	0.1880	-0.0136	0.5473	0.0232	0.1923	-0.0137
	0.0230	0.0013	0.0136	-0.0009	0.0232	0.0013	0.0138	-0.0009
	0.1880	0.0136	1.0864	0.0000	0.1923	0.0138	1.0879	-0.0002
	-0.0136	-0.0009	0.0000	0.0025	-0.0137	-0.0009	-0.0002	0.0025
Stiffness matrix x 10^{-6}	2.9948	0.4492	-2.9948	0.4492	3.0078	0.4518	-3.0033	0.4510
	0.4492	0.0898	-0.4492	0.0449	0.4518	0.0903	-0.4508	0.0455
	-2.9948	-0.4492	5.9896	0.0000	-3.0033	-0.4508	5.9863	-0.0034
	0.4492	0.0449	0.0000	1.7969	0.4510	0.0455	-0.0034	1.7940

Table 3.5 Comparision for a beam (4x4) (structural damping)

	η= 0.05							
	Actual values				Identified values			
Mass matrix	0.5432	0.0230	0.1880	-0.0136	0.5421	0.0229	0.1959	-0.0134
	0.0230	0.0013	0.0136	-0.0009	0.0229	0.0012	0.0141	-0.0009
	0.1880	0.0136	1.0864	0.0000	0.1959	0.0141	1.1111	-0.0003
	-0.0136	-0.0009	0.0000	0.0025	-0.0134	-0.0009	-0.0003	0.0025
Stiffness matrix x 10^{-6}	2.9948	0.4492	-2.9948	0.4492	2.9617	0.4436	-2.9586	0.4452
	0.4492	0.0898	-0.4492	0.0449	0.4436	0.0887	-0.4392	0.0450
	-2.9948	-0.4492	5.9896	0.0000	-2.9586	-0.4392	5.9556	-0.0001
	0.4492	0.0449	0.0000	1.7969	0.4452	0.0450	-0.0001	1.7748

Table 3.6a Comparision for a beam (6x6) (structural damping)

η = 0.01					
Actual mass matrix					
0.3621	0.0102	0.1254	-0.0060	0.0000	0.0000
0.0102	0.0004	0.0060	-0.0003	0.0000	0.0000
0.1254	0.0060	0.7243	0.0000	0.1254	-0.0060
-0.0060	-0.0003	0.0000	0.0007	0.0060	-0.0003
0.0000	0.0000	0.1254	0.0060	0.7243	0.0000
0.0000	0.0000	-0.0060	-0.0003	0.0000	0.0007
Identified mass matrix					
0.3647	0.0103	0.1274	-0.0061	0.0013	0.0000
0.0103	0.0004	0.0061	-0.0003	0.0000	0.0000
0.1274	0.0061	0.7291	0.0000	0.1250	-0.0061
-0.0061	-0.0003	0.0000	0.0007	0.0060	-0.0003
0.0013	0.0000	0.1250	0.0060	0.7273	0.0000
0.0000	0.0000	-0.0061	-0.0003	0.0000	0.0007

...contd..

Table 3.6b Comparision for a beam (6x6) (Structural damping)

$\eta = 0.01$					
Actual stiffness matrix $x10^{-7}$					
1.0107	0.1011	-1.0107	0.1011	0.0000	0.0000
0.1011	0.0135	-0.1011	0.0067	0.0000	0.0000
-1.0107	-0.1011	2.0215	0.0000	-1.0107	0.1011
0.1011	0.0067	0.0000	0.0270	-0.1011	0.0067
0.0000	0.0000	-1.0107	-0.1011	2.0215	0.0000
0.0000	0.0000	0.1011	0.0067	0.0000	0.0270
Identified stiffness matrix $x10^{-7}$					
1.0134	0.1013	-1.0147	0.1013	0.0018	-0.0002
0.1013	0.0135	-0.1014	0.0067	0.0001	0.0000
-1.0147	-0.1014	2.0316	0.0000	-1.0186	0.1017
0.1013	0.0067	0.0000	0.0270	-0.1016	0.0067
0.0018	0.0001	-1.0186	-0.1016	2.0344	0.0003
-0.0002	0.0000	0.1017	0.0067	0.0003	0.0271

Table 3.7a Comparision for a beam (6x6) (structural damping)

η = 0.05					
Actual mass matrix					
0.3621	0.0102	0.1254	-0.0060	0.0000	0.0000
0.0102	0.0004	0.0060	-0.0003	0.0000	0.0000
0.1254	0.0060	0.7243	0.0000	0.1254	-0.0060
-0.0060	-0.0003	0.0000	0.0007	0.0060	-0.0003
0.0000	0.0000	0.1254	0.0060	0.7243	0.0000
0.0000	0.0000	-0.0060	-0.0003	0.0000	0.0007
Identified mass matrix					
0.3660	0.0102	0.1284	-0.0059	-0.0071	-0.0001
0.0102	0.0004	0.0062	-0.0003	-0.0002	0.0000
0.1284	0.0062	0.7316	-0.0002	0.1220	-0.0062
-0.0059	-0.0003	-0.0002	0.0007	0.0061	-0.0003
-0.0071	-0.0002	0.1220	0.0061	0.7021	-0.0002
-0.0001	0.0000	-0.0062	-0.0003	-0.0002	0.0007

...contd..

Table 3.7b Comparision for a beam (6x6) (structural damping)

η=0.05					
Actual stiffness matrix x 10^7					
1.0107	0.1011	-1.0107	0.1011	0.0000	0.0000
0.1011	0.0135	-0.1011	0.0067	0.0000	0.0000
-1.0107	-0.1011	2.0215	0.0000	-1.0107	0.1011
0.1011	0.0067	0.0000	0.0270	-0.1011	0.0067
0.0000	0.0000	-1.0107	-0.1011	2.0215	0.0000
0.0000	0.0000	0.1011	0.0067	0.0000	0.0270
Identified stiffness matrix x 10^7					
0.9877	0.0987	-1.0007	0.0961	-0.0060	-0.0015
0.0987	0.0132	-0.0984	0.0064	-0.0027	0.0000
-1.0007	-0.0984	1.9824	-0.0006	-0.9595	0.0960
0.0961	0.0064	-0.0006	0.0256	-0.0954	0.0062
-0.0060	-0.0027	-0.9595	-0.0954	1.9375	0.0015
-0.0015	0.0000	0.0960	0.0062	0.0015	0.0251

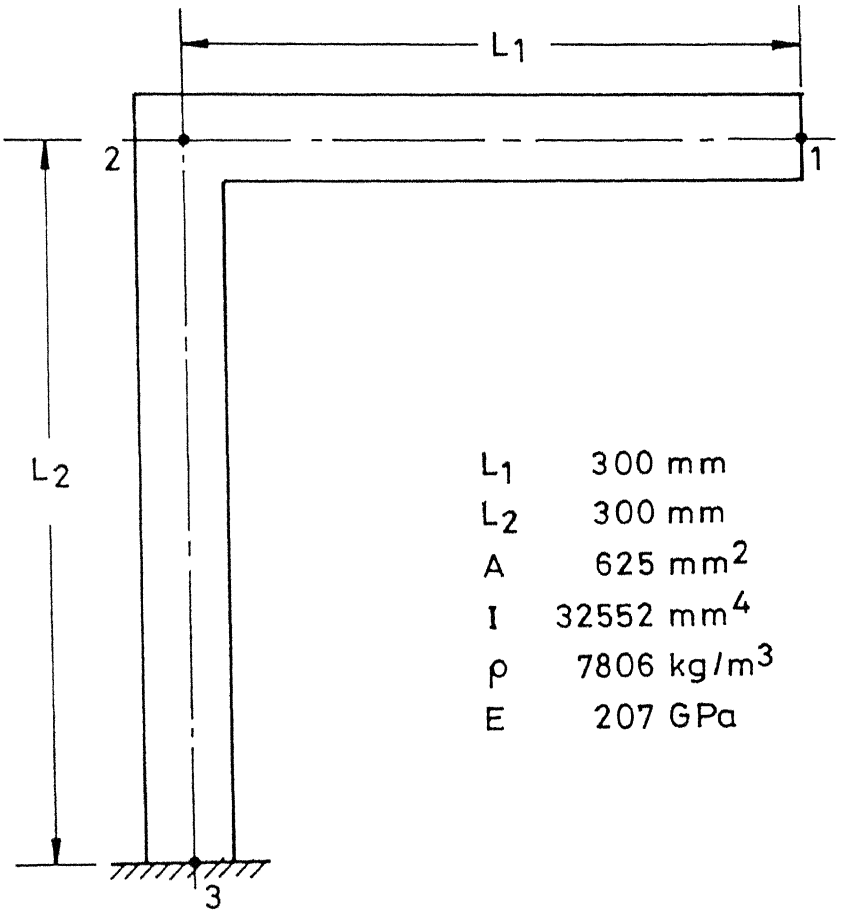

Fig. 3.4 L-Frame structure.

Table 3.8a Comparision for L-Frame (6x6) (structural damping)

η = 0.01					
Actual mass matrix					
0.4875	0.0000	0.0000	0.2438	0.0000	0.0000
0.0000	0.5432	0.0230	0.0000	0.1880	-0.0136
0.0000	0.0230	0.0013	0.0000	0.0136	-0.0009
0.2438	0.0000	0.0000	1.0307	0.0000	-0.0230
0.0000	0.1880	0.0136	0.0000	1.0307	-0.0230
0.0000	-0.0136	-0.0009	-0.0230	-0.0230	0.0025
Identified mass matrix					
0.4881	-0.0017	0.0000	0.2473	0.0001	0.0000
-0.0017	0.5450	0.0230	-0.0027	0.1950	-0.0136
0.0000	0.0230	0.0012	0.0002	0.0142	-0.0009
0.2473	-0.0027	-0.0002	1.0315	-0.0017	-0.0227
0.0001	0.1950	0.0142	-0.0017	0.9874	-0.0228
0.0000	-0.0136	-0.0009	-0.0227	-0.0228	0.0025

...contd...

Table 3.8b Comparision for L-Frame (6x6) (Structural damping)

$\eta = 0.01$					
Actual stiffness matrix x 10^8					
4.3125	0.0000	0.0000	-4.3125	0.0000	0.0000
0.0000	0.0300	0.0045	0.0000	-0.0300	0.0045
0.0000	0.0045	0.0009	0.0000	-0.0045	0.0005
-4.3125	0.0000	0.0000	4.3425	0.0000	-0.0050
0.0000	-0.0300	-0.0045	0.0000	4.3425	-0.0045
0.0000	0.0045	0.0005	-0.0050	-0.0045	0.0018
Identified stiffness matrix x10^8					
4.3003	-0.0005	-0.0001	-4.3000	-0.0030	-0.0001
-0.0005	0.0291	0.0043	0.0006	-0.0175	0.0044
-0.0001	0.0043	0.0009	0.0001	-0.0020	0.0004
-4.3000	0.0006	0.0001	4.3295	0.0027	-0.0043
-0.0030	-0.0175	-0.0020	0.0027	4.0316	-0.0032
-0.0001	0.0044	0.0004	-0.0043	-0.0032	0.0018

Table 3.9a Comparision for L-Frame (Structural damping)

η= 0.05					
Actual mass matrix					
0.4875	0.0000	0.0000	0.2438	0.0000	0.0000
0.0000	0.5432	0.0230	0.0000	0.1880	-0.0136
0.0000	0.0230	0.0013	0.0000	0.0136	-0.0009
0.2438	0.0000	0.0000	1.0307	0.0000	-0.0230
0.0000	0.1880	0.0136	0.0000	1.0307	-0.0230
0.0000	-0.0136	-0.0009	-0.0230	-0.0230	0.0025
Identified mass matrix					
0.4999	-0.0040	-0.0002	0.2554	0.0083	0.0002
-0.0040	0.5272	0.0223	-0.0090	0.2005	-0.0132
-0.0002	0.0223	0.0012	-0.0012	0.0146	-0.0008
0.2554	-0.0090	-0.0012	1.0054	-0.0546	-0.0188
0.0083	0.2005	0.0146	-0.0546	0.8146	-0.0158
0.0002	-0.0132	-0.0008	-0.0188	-0.0158	0.0020

...Contd...

Table 3.9b Comparision for L-Frame (6x6) (Structural damping)

η= 0.05					
Actual stiffness matrix x 10^8					
4.3125	0.0000	0.0000	-4.3125	0.0000	0.0000
0.0000	0.0300	0.0045	0.0000	-0.0300	0.0045
0.0000	0.0045	0.0009	0.0000	-0.0045	0.0005
-4.3125	0.0000	0.0000	4.3425	0.0000	-0.0050
0.0000	-0.0300	-0.0045	0.0000	4.3425	-0.0045
0.0000	0.0045	0.0005	-0.0050	-0.0045	0.0018
Identified stiffness matrix x 10^8					
4.2850	0.0054	0.0014	-4.2826	-0.1389	-0.0002
0.0054	0.0258	0.0037	-0.0050	0.0389	0.0039
0.0014	0.0037	0.0007	-0.0015	0.0076	0.0004
-4.2826	-0.0050	-0.0015	4.3080	0.1226	-0.0036
-0.1389	0.0389	0.0076	0.1226	3.2450	0.0074
-0.0002	0.0039	0.0004	-0.0036	0.0074	0.0015

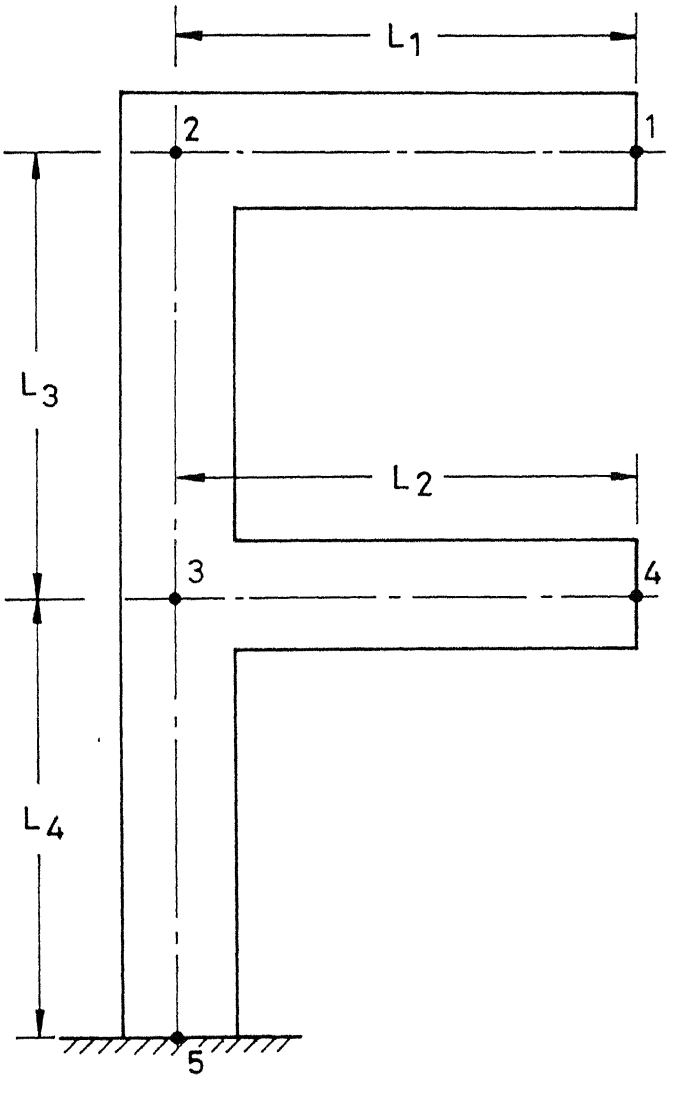

L_1	300 mm
L_2	300 mm
L_3	300 mm
L_4	300 mm
A	625 mm^2
I	32552 mm^4
ρ	7806 kg/m^3
E	207 GPa

Fig. 3.5 F-Frame structure.

Table 3.10a Comparision for F-Frame (12x12) (Structural Damping)

η = 0.01

Actual mass matrix

0.4879	0.0000	0.0000	0.2439	0.0000	0.0000	0.0000	0.0000	0.0000	0.0000	0.0000	0.0000
0.0000	0.5436	0.0230	0.0000	0.1882	-0.0136	0.0000	0.0000	0.0000	0.0000	0.0000	0.0000
0.0000	0.0230	0.0013	0.0000	0.0136	-0.0009	0.0000	0.0000	0.0000	0.0000	0.0000	0.0000
0.2439	0.0000	0.0000	1.0315	0.0000	-0.0230	0.1882	0.0000	0.0136	0.0000	0.0000	0.0000
0.0000	0.1882	0.0136	0.0000	1.0315	-0.0230	0.0000	0.2439	0.0000	0.0000	0.0000	0.0000
0.0000	-0.0136	-0.0009	-0.0230	-0.0230	0.0025	-0.0136	0.0000	-0.0009	0.0000	0.0000	0.0000
0.0000	0.0000	0.0000	0.1882	0.0000	-0.0136	1.5751	0.0000	0.0000	0.2439	0.0000	0.0000
0.0000	0.0000	0.0000	0.0000	0.2439	0.0000	0.0000	1.5194	-0.0230	0.0000	0.1882	0.0136
0.0000	0.0000	0.0000	0.0136	0.0000	-0.0009	0.0000	-0.0230	0.0038	0.0000	-0.0136	-0.0009
0.0000	0.0000	0.0000	0.0000	0.0000	0.0000	0.2439	0.0000	0.0000	0.4879	0.0000	0.0000
0.0000	0.0000	0.0000	0.0000	0.0000	0.0000	0.0000	0.1882	-0.0136	0.0000	0.5436	0.0230
0.0000	0.0000	0.0000	0.0000	0.0000	0.0000	0.0000	0.0136	-0.0009	0.0000	0.0230	0.0013

Identified mass matrix

0.4979	0.0004	-0.0000	0.2540	-0.0016	0.0001	-0.0064	0.0006	0.0000	-0.0024	-0.0040	-0.0001
0.0004	0.3381	0.0143	-0.0489	0.1044	-0.0048	-0.2185	0.0233	-0.0034	-0.0782	0.0658	0.0027
-0.0000	0.0143	0.0009	-0.0022	0.0088	-0.0005	-0.0091	-0.0003	-0.0001	-0.0031	0.0027	0.0001
0.2540	-0.0489	-0.0022	1.0446	-0.0362	-0.0212	0.1394	-0.0037	0.0140	-0.0219	0.0051	0.0001
-0.0016	0.1044	0.0088	-0.0362	0.9102	-0.0163	-0.0928	0.1534	0.0028	-0.0237	0.0257	-0.0003
0.0001	-0.0048	-0.0005	-0.0212	-0.0163	0.0021	-0.0051	0.0023	-0.0010	0.0030	-0.0024	-0.0000
-0.0064	-0.2185	-0.0091	0.1394	-0.0928	-0.0051	1.3824	0.0193	-0.0032	0.2050	0.0440	0.0019
0.0006	0.0233	-0.0003	-0.0037	0.1534	0.0023	0.0193	1.3739	-0.0192	0.0200	0.1663	0.0115
0.0000	-0.0034	-0.0001	0.0140	0.0028	-0.0010	-0.0032	-0.0192	0.0035	-0.0015	-0.0116	-0.0008
-0.0024	-0.0782	-0.0031	-0.0219	-0.0237	0.0030	0.2050	0.0200	-0.0015	0.4361	0.0121	0.0007
-0.0040	0.0658	0.0027	0.0051	0.0257	-0.0024	0.0440	0.1663	-0.0116	0.0121	0.4944	0.0209
-0.0001	0.0027	0.0001	0.0001	-0.0003	-0.0000	0.0019	0.0115	-0.0008	0.0007	0.0209	0.0011

Table 3.10b Comparision for F-Frame (12x12) (Structural Damping)

η = 0.01

Actual stiffness matrix x 1.0E-8

4.3125	0.0000	0.0000	-4.3125	0.0000	0.0000	0.0000	0.0000	0.0000	0.0000	0.0000	0.0000
0.0000	0.0299	0.0045	0.0000	-0.0299	0.0045	0.0000	0.0000	0.0000	0.0000	0.0000	0.0000
0.0000	0.0045	0.0009	0.0000	-0.0045	0.0004	0.0000	0.0000	0.0000	0.0000	0.0000	0.0000
-4.3125	0.0000	0.0000	4.3424	0.0000	-0.0045	-0.0299	0.0000	-0.0045	0.0000	0.0000	0.0000
0.0000	-0.0299	-0.0045	0.0000	4.3424	-0.0045	0.0000	-4.3125	0.0000	0.0000	0.0000	0.0000
0.0000	0.0045	0.0004	-0.0045	-0.0045	0.0018	0.0045	0.0000	0.0004	0.0000	0.0000	0.0000
0.0000	0.0000	0.0000	-0.0299	0.0000	0.0045	4.3724	0.0000	0.0000	-4.3125	0.0000	0.0000
0.0000	0.0000	0.0000	0.0000	-4.3125	0.0000	0.0000	8.6549	-0.0045	0.0000	-0.0299	-0.0045
0.0000	0.0000	0.0000	-0.0045	0.0000	0.0004	0.0000	-0.0045	0.0027	0.0000	0.0045	0.0004
0.0000	0.0000	0.0000	0.0000	0.0000	0.0000	-4.3125	0.0000	0.0000	4.3125	0.0000	0.0000
0.0000	0.0000	0.0000	0.0000	0.0000	0.0000	0.0000	-0.0299	0.0045	0.0000	0.0299	0.0045
0.0000	0.0000	0.0000	0.0000	0.0000	0.0000	0.0000	-0.0045	0.0004	0.0000	0.0045	0.0009

Identified stiffness matrix x 1.0E-8

4.3534	-0.0006	-0.0002	-4.3533	0.0292	-0.0000	-0.0078	-0.0428	-0.0000	0.0077	0.0001	0.0000
-0.0006	0.0287	0.0044	0.0004	-0.0312	0.0046	-0.0049	0.0047	0.0000	0.0030	0.0003	-0.0000
-0.0002	0.0044	0.0009	-0.0000	-0.0058	0.0005	-0.0006	0.0007	0.0001	0.0006	-0.0000	-0.0000
-4.3533	0.0004	-0.0000	4.3816	-0.0457	-0.0041	-0.0190	0.0445	-0.0038	-0.0110	-0.0003	-0.0002
0.0292	-0.0312	-0.0058	-0.0457	4.3606	-0.0009	-0.0080	-4.3308	0.0048	0.0165	-0.0007	-0.0012
-0.0000	0.0046	0.0005	-0.0041	-0.0009	0.0017	0.0034	0.0005	0.0003	0.0010	0.0000	0.0000
-0.0078	-0.0049	-0.0006	-0.0190	-0.0080	0.0034	3.9404	-0.0220	-0.0008	-3.8850	-0.0007	-0.0000
-0.0428	0.0047	0.0007	0.0445	-4.3308	0.0005	-0.0220	8.1347	-0.0051	0.0217	-0.0313	-0.0049
-0.0000	0.0000	0.0001	-0.0038	0.0048	0.0003	-0.0008	-0.0051	0.0025	0.0003	0.0046	0.0005
0.0077	0.0030	0.0006	-0.0110	0.0165	0.0010	-3.8850	0.0217	0.0003	3.8883	0.0007	0.0002
0.0001	0.0003	-0.0000	-0.0003	-0.0007	0.0000	-0.0007	-0.0313	0.0046	0.0007	0.0293	0.0044
0.0000	-0.0000	-0.0000	-0.0002	-0.0012	0.0000	-0.0000	-0.0049	0.0005	0.0002	0.0044	0.0009

Table 3.11 Comparision for a discrete system (2x2) (viscous damping)

$\beta' = 1.0 \times 10^{-6}$				
	Actual values		Identified values	
Mass matrix	1.0000	0.0000	1.0303	0.0473
	0.0000	2.0000	0.0473	1.9397
Stiffness matrix $\times 10^{-4}$	3.5000	-2.0000	3.5070	-1.9755
	-2.0000	2.0000	-1.9755	1.9704

Table 3.12 Comparision for an axial rod (2x2)
(viscous damping)

	$\beta' = 1.0 \times 10^{-6}$			
	Actual values		Identified values	
Mass matrix	5.1071	2.5535	5.0786	2.5252
	2.5535	10.2143	2.5252	10.1591
Stiffness matrix $\times 10^{-8}$	4.1250	-4.1250	4.1122	-4.1188
	-4.1250	8.2500	-4.1188	8.2246

Table 3.13 Comparision for a beam (4x4) (viscous damping)

	$\beta' = 1.0 \times 10^{-6}$							
	Actual values				Identified values			
Mass matrix	0.5432	0.0230	0.1880	-0.0136	0.5148	0.0217	0.1698	-0.0128
	0.0230	0.0013	0.0136	-0.0009	0.0217	0.0012	0.0126	-0.0009
	0.1880	0.0136	1.0864	0.0000	0.1698	0.0126	1.0476	0.0005
	-0.0136	-0.0009	0.0000	0.0025	-0.0128	-0.0009	0.0005	0.0025
Stiffness matrix $\times 10^{6}$	2.9948	0.4492	-2.9948	0.4492	2.9678	0.4463	-2.9566	0.4476
	0.4492	0.0898	-0.4492	0.0450	0.4463	0.0894	-0.4472	0.0444
	-2.9948	-0.4492	5.9896	0.0000	-2.9566	-0.4472	5.8903	0.0019
	0.4492	0.0450	0.0000	0.1797	0.4476	0.0444	0.0019	0.1798

Table 3.14a Comparision for L-Frame (6x6) (viscous damping)

$\beta' = 1.0 \times 10^{-6}$					
Actual mass matrix					
0.4875	0.0000	0.0000	0.2438	0.0000	0.0000
0.0000	0.5432	0.0230	0.0000	0.1880	-0.0136
0.0000	0.0230	0.0013	0.0000	0.0136	-0.0009
0.2438	0.0000	0.0000	1.0307	0.0000	-0.0230
0.0000	0.1880	0.0136	0.0000	1.0307	-0.0230
0.0000	-0.0136	-0.0009	-0.0230	-0.0230	0.0025
Identified mass matrix					
0.5378	-0.0037	-0.0001	0.2302	-0.0002	0.0003
-0.0037	0.5378	0.0230	0.0069	0.1324	-0.0132
-0.0001	0.0230	0.0013	-0.0003	0.0125	-0.0009
0.2302	0.0069	-0.0003	0.9766	-0.0359	-0.0237
-0.0002	0.1324	0.0125	-0.0359	0.8004	-0.0190
0.0003	-0.0132	-0.0009	-0.0237	-0.0190	0.0025

Table 3.14b Comparision for L-Frame (6x6) (viscous damping)

$\beta' = 1.0 \times 10^{6}$					
Actual stiffness matrix $\times 10^{8}$					
4.3125	0.0000	0.0000	-4.3125	0.0000	0.0000
0.0000	0.0300	0.0045	0.0000	-0.0300	0.0045
0.0000	0.0045	0.0009	0.0000	-0.0045	0.0005
-4.3125	0.0000	0.0000	4.3425	0.0000	-0.0050
0.0000	-0.0300	-0.0045	0.0000	4.3425	-0.0045
0.0000	0.0045	0.0005	-0.0050	-0.0045	0.0018
Identified stiffness matrix $\times 10^{8}$					
4.3709	0.0071	0.0041	-4.3719	0.1114	0.0009
0.0071	0.0301	0.0045	-0.0077	0.0113	0.0047
0.0014	0.0045	0.0009	-0.0015	0.0036	0.0005
-4.3719	-0.0077	-0.0015	4.4028	-0.1159	-0.0055
0.1114	0.0113	0.0036	-0.1159	3.2088	0.0007
0.0009	0.0047	0.0005	-0.0055	0.0007	0.0018

REFERENCES

1. Kundra, T.K., 'Studies in Identification and Modification of Dynamic Mechanical Systems', Ph.D. Thesis, Dept. of Mech. Engg., I.I.T., Delhi, April 1986.

2. Vepa, K., 'Optimal Identification of Vibrating Structures', International Modal Analysis Conference and Exhibit (IMAC2), Orlando, Florida, Feb. 1984.

3. Ewins, D.J., 'Modal Testing : Theory and Practice', Research Studies Press Ltd., John Wiley and Sons Inc., 1984.

4. Kennedy, C.C., and Pancu, C.D.P., 'Use of Vectors in Vibration Measurement and Analysis', J. Aeronautical Sciences, Vol. 14, No. 11, 1947, pp. 603-625.

5. Bishop, R.E.D., and Gladwell, G.M.L., 'An Investigation into the Theory of Resonance Testing', Proc Roy Soc Phil Trans 255(A) 241, 1963.

6. Salter, J.P., 'Steady State Vibration', Kenneth Mason Press, 1969.

7. Allemang, R.J., 'Experimental Modal Analysis Bibliography', Proc. IMAC2, Feb. 1984.

8. Mitchell, L.D., and Mitchell, L.D.,'Modal Analysis Bibliography - An update- 1980-1983' Proc. IMAC2, Feb. 1984.

9. Flannelly, W.G., McGarvey, J.H., and Berman, A., 'A Theory of Identification of the Parameters in the Equations of Motions of a Structure through Dynamic Testing', Papers Presented at the Symposium on Structural Dynamics, University of Technology, Loughborough, U.K., March 23-25, 1970.

10. Berman, A., 'Determining Structural Parameters from Dynamic Testing', The Shock and Vibration Digest, 7(1), Jan. 1975.

11. Zaveri, 'Modal Analysis of Large Structures - Multiple Exciter Systems', Bruel and Kjaer, April 1985.

12. Meirovitch, L., 'Elements of Vibration Analysis', McGraw-Hill International Editions, 1986.